Low-temperature synthesis of ZnO nanoparticles by solid-state pyrolytic reaction

2003 Nanotechnology 14 11

(http://iopscience.iop.org/0957-4484/14/1/303)

INSTITUTE OF PHYSICS PUBLISHING NANOTECHNOLOGY
Nanotechnology **14** (2003) 11–15 PII: S0957-4484(03)39929-5

Low-temperature synthesis of ZnO nanoparticles by solid-state pyrolytic reaction

Zhijian Wang[1,2], Haiming Zhang[1,2], Ligong Zhang[1,2], Jinshan Yuan[1,2,4], Shenggang Yan[3] and Chunyan Wang[3]

[1] Laboratory of Excited State Processes, Chinese Academy of Sciences, Changchun 130021, China
[2] Changchun Institute of Optics, Fine Mechanics and Physics, Chinese Academy of Sciences, Changchun 130021, China
[3] School of Chemical Engineering, Dalian University of Technology, Dalian 116012, China

E-mail: yjswls@mail.jl.cn

Received 24 July 2002, in final form 14 October 2002
Published 3 December 2002
Online at stacks.iop.org/Nano/14/11

Abstract
A new method for the growth of high-quality ZnO nanoparticles is presented here; it is a novel, low-cost, and easy operation. This approach, using solid-state heat decomposition at low temperature, allows one to produce ZnO nanoparticles with relatively high dispersivity. The optical properties of the ZnO nanoparticles have been investigated. It is demonstrated that ZnO nanoparticles show strong ultraviolet emission, while the low-energy visible emission is nearly fully quenched at room temperature. This is a result of the high quality of the ZnO. X-ray diffraction patterns reveal that the ZnO nanoparticles have polycrystalline hexagonal wurtzite structure. The Raman spectrum shows a typical resonant multi-phonon form for the ZnO nanoparticles. Similar synthesis routes for other metal oxide nanoparticles may be possible.

1. Introduction

In recent years, intensive development of nanocrystalline materials and in nanotechnology has occurred worldwide. The intensive investigations were stimulated by several application areas being envisaged for these new classes of material. As a wide-band-gap ($E_g = 3.37$ eV) semiconductor, ZnO has been widely studied—in varistors, transparent conductors, transparent UV-protection films, chemical sensors, and so on [1–4]. In the past decade, various methods have been employed to produce ZnO [5–10], including vapour decomposition, precipitation, and thermal decomposition. Despite recent advances, commercial exploitation of ZnO nanoparticles is currently limited by the high synthesis costs and visible emission characteristics.

In most of the previous work, visible emission always dominates the photoluminescence (PL) spectra of ZnO nanocrystallites [5, 7, 11]. PL spectra of ZnO nanocrystallites with purely strong UV emission have scarcely been reported [12]. Here, we report a simple, rapid, low-cost, and low-temperature solid-state thermal decomposition process for the synthesis of ZnO nanoparticles with an adjustable size from 8 to 35 nm. The low-temperature nature can greatly decrease the constraints (vacancies, heat defects, etc) on combining desirable characteristics of ZnO nanoparticles. The as-prepared ZnO nanoparticles showed a strong UV emission peak at around 388 nm, while the visible emission was nearly fully quenched. The strong UV emission is attributed to the fine quality of the ZnO nanoparticles.

2. Experimental section

2.1. Chemicals

The zinc acetate dihydrate (99.5%) $Zn(CH_3COO)_2{\cdot}2H_2O$, sodium hydrogen carbonate (99.5%) $NaHCO_3$, and ethanol (99.9%) were all from Beijing Chemical Agent Corporation. All chemicals were directly used without special treatment.

[4] Author to whom any correspondence should be addressed.

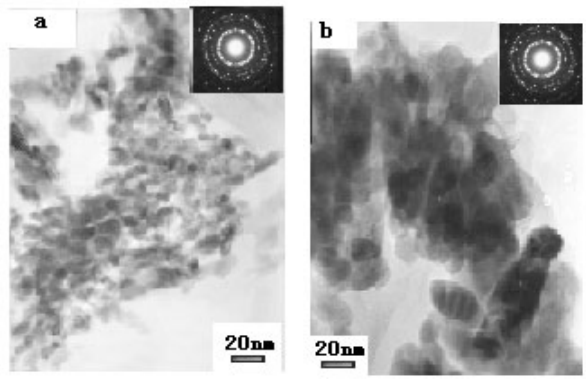

Figure 1. TEM images of ZnO nanoparticles: (a) thermal decomposition at 160 °C for 2 h then aging at 180 °C for 16 h; (b) thermal decomposition at 300 °C for 3 h.

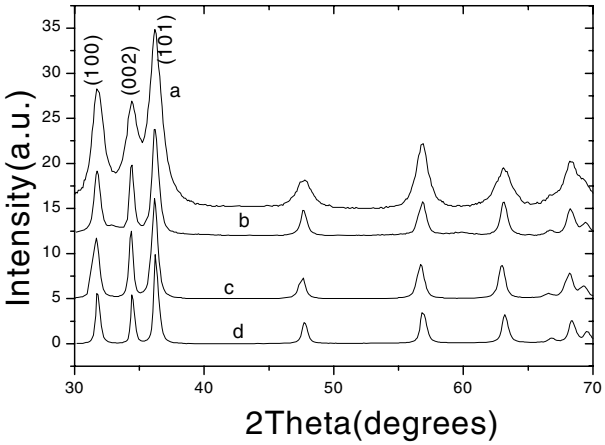

Figure 2. Powder x-ray diffraction spectra of ZnO nanoparticles. (a) Heated at 160 °C for 2 h, then aged at 180 °C for 16 h. (b–d) Heated at 200, 250, and 300 °C, respectively, for 3 h.

2.2. Sample preparation

A typical synthesis procedure is as follows. 2.2 g (10 mmol) of $Zn(CH_3COO)_2{\cdot}2H_2O$ and 2 g (23.8 mmol) of $NaHCO_3$ are mixed at room temperature. The mixture is pyrolysed at the reaction temperature. The $Zn(CH_3COO)_2{\cdot}2H_2O$ is changed into ZnO nanoparticles, while the $NaHCO_3$ is changed into CH_3COONa and eventually washed away with deionized water. Consequently, white ZnO nanoparticles are obtained, through the thermal decomposition process. The particle sizes can be controlled by adjusting the pyrolytic temperature.

2.3. Apparatus

The transmission electron microscopy (TEM) images and selected-area electron diffraction (SAED) patterns were taken on a JEOL-2010 TEM operated at 200 kV. X-ray powder diffraction (XRD) was used to investigate the ZnO powders; we used a Rigaku RU-200B Rotaflex diffraction meter using Cu Kα radiation and $\lambda = 1.5406$ Å. Absorption measurements were performed using a UV-360 spectra-recording photometer (Shimadzu). X-ray photoelectron spectrometry (XPS) measurements were performed on a Kratos AXIS HS instrument, using a monochromatized Al Kα source and a 20 eV pass energy. Infrared (IR) absorption spectra were collected using a Shimadzu FT-IR 8200D spectrometer. The Raman spectra measurements were carried out using a microlaser Raman spectrometer. The PL spectra were recorded with a Hitachi MPF-4 fluorescence spectrophotometer. The spectra were obtained by exciting the sample with a 325 nm wavelength at room temperature. After completion of the reaction, TEM samples were prepared by placing a drop of the dilute ethanol solution on the surface of a copper grid (250 mesh).

3. Results and discussion

In the solid-state thermal decomposition process, the by-products play an important role in controlling particle growth and agglomeration. The method proposed here is focused on a strategy for separating these nanoparticles using the by-product CH_3COONa, which can distribute on the ZnO nanoparticle surfaces, preventing them from agglomerating. Moreover, such nanocomposite structures can be converted into nanoparticles by dissolution of CH_3COONa.

Figure 1 shows TEM images and corresponding SAED patterns. The image at 200×10^3 times magnification indicates that the ZnO nanoparticles consistently show crystal structure with unchanging morphology. The typical morphology for the ZnO is small rod-like shapes, which indicate the growth of nanoparticles along a certain direction. The agglomeration of particles in TEM may be arising from solvent volatile agglomeration that occurred when we prepared the TEM samples. It is well known that the chemical reaction is always composed of four stages, which are diffusion, reaction, nucleation, and growth. Experimental results clearly indicated the kinetic mechanism of the evolution of ZnO nanoparticles. The growth process of ZnO nanoparticles was controlled by diffusion. The details of the synthesis procedures and kinetic mechanism of evolution for ZnO nanoparticles produced by low-temperature solid-state pyrolytic reaction will be published elsewhere. As is well known, particle size distribution is an important feature of powders. In this paper, the particle sizes were controlled by selecting different pyrolytic temperatures. The particle sizes are distributed over a range of 8–35 nm. The x-ray diffraction patterns for the various particle sizes of ZnO are shown in figure 2. Three pronounced ZnO peaks, (100), (002), and (101), appear at $2\theta = 31.86°$, $34.68°$, and $36.36°$, respectively. These results indicate that ZnO has a polycrystalline hexagonal wurtzite structure. Figure 2(a) shows the sample heated at 160 °C for 2 h and then aged at 180 °C for 16 h. In contrast, figure 2(d) shows the sample formed by decomposition at 300 °C for 3 h. The dimensions of the ZnO nanoparticles calculated from the widths of the major diffraction peaks observed in figure 2 through the Scherrer formula [13] are listed in table 1. The calculated values for samples (a) and (d) correspond to the TEM values.

In general, absorption spectra probe the crystallite internal molecular orbital and provide information concerning size and particle composition [14]. Optical absorption spectra for ZnO ethanol solutions are presented in figure 3. Two features are clearly visible from these spectra. First, the spectra exhibit distinct exciton absorption [7], second, as the particle sizes

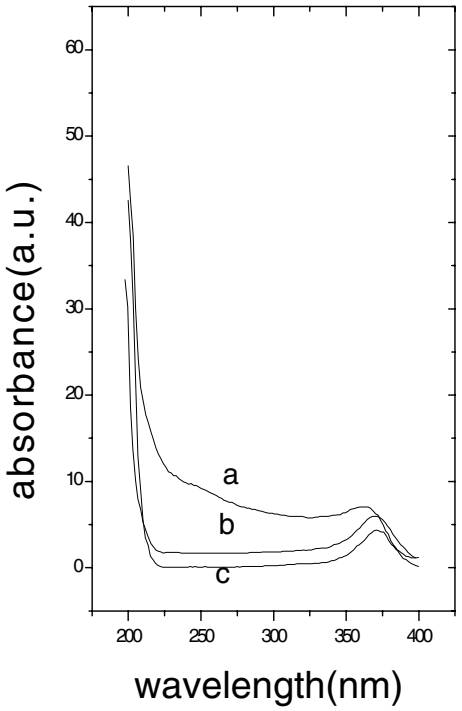

Figure 3. Absorption spectra of ZnO nanoparticles; thermal decomposition at different temperatures for 3 h: (a) 200 °C, (b) 250 °C, and (c) 300 °C.

Table 1. Crystallite sizes along (101) zone axes.

Sample	FWHM (deg)	Particle sizes (nm)
a	1.07	7.8
b	0.49	17
c	0.46	18
d	0.35	24

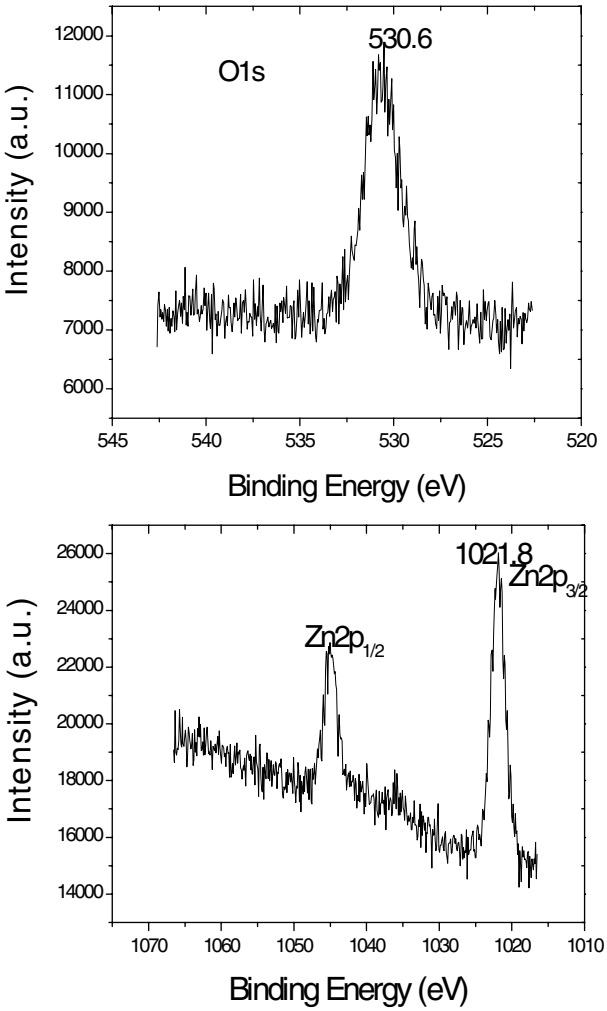

Figure 4. O 1s and Zn 2p XPS spectra of ZnO nanoparticles.

grow, the excitonic absorption peaks gradually shift from 360 to 375 nm. Both effects can be understood in terms of the quantum size effect upon particle size growth. In order to estimate the diameter of the ZnO nanoparticles, from the excitonic absorption peak shift, the Brus effective mass model was used [15]. During the ZnO nanoparticle formation, each particle is surrounded by the by-product CH_3COONa phase. Because the volume fraction of the product phase is less that the percolation limit, the formation of separated ZnO nanoparticles is guaranteed by the solid-state nature of the reaction. An interesting feature can also be found from the absorption spectra: there is a strong absorption around 5.6355 eV. Future study of the origin of the strong absorption around 5.6355 eV should lead to a more complete description of the structural properties of ZnO nanoparticles, which may help us to establish the origin of the absorption.

XPS data for the ZnO nanoparticles are shown in figure 4. The binding energies of O(1s), Zn($2p_{1/2}$), and ZnO($2p_{3/2}$) provided a fairly complete picture of the sample powder. The ZnO($2p_{3/2}$) XPS peak that appears at 1021.8 eV coincides with the findings for ZnO. The O(1s) peak at 530.6eV is attributed to oxide ions in ZnO. A full survey scan did not reveal other element peaks. These results indicate that pure ZnO nanoparticles have formed. Compared to those for other methods for synthesizing ZnO powders, the conditions for the reaction are very moderate. In order to further confirm that we have obtained fine-quality ZnO nanoparticles, supplementary experiments have been carried out on IR spectra and Raman scattering. Figure 5 shows a typical IR spectrum for ZnO nanoparticles. The peak around 450 cm^{-1} shows a distinct stretching mode of crystal ZnO: some absorption water on the surface of ZnO; but no peaks corresponding to other compounds are seen. If there is adsorption of sodium (zinc) acetate on the surface of the ZnO particles, a distinct carbonyl peak around 1740 cm^{-1} should appear in the IR spectrum. Figure 6 shows a typical Raman spectrum for the ZnO nanoparticles. The Raman spectrum consisted of three sharp lines. Our measurement of the frequency shift of the 1LO phonon is 584.7 cm^{-1}; this result is consistent with the value 585 cm^{-1} previously reported [16]. The 2LO and 3LO phonons were also observed. This result indicated that the ZnO nanoparticles are of fine quality. To our knowledge, multiple-phonon scattering processes have been previously observed only in ZnO bulk crystal materials [17]. For ZnO nanoparticles prepared by solid-state pyrolytic reaction at low temperature, resonant Raman scattering has not previously been reported in the literature.

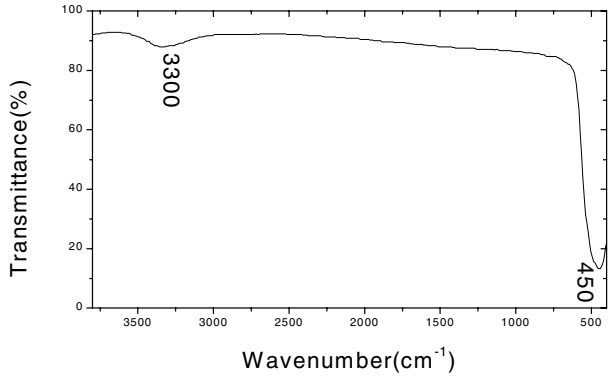

Figure 5. Typical IR spectra of ZnO nanoparticles.

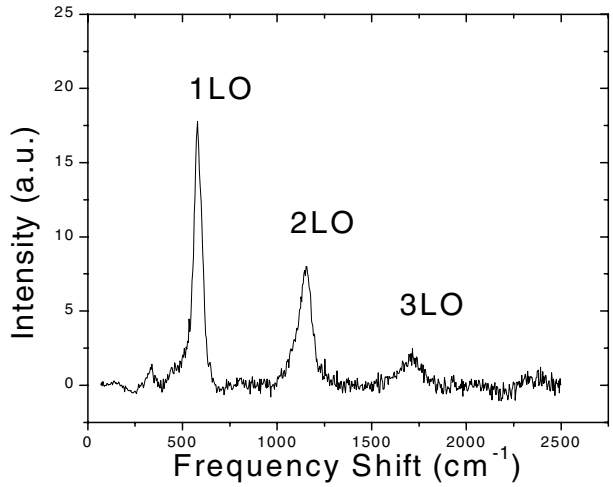

Figure 6. A resonant Raman spectrum of ZnO excited with a 325 nm He–Cd laser at room temperature.

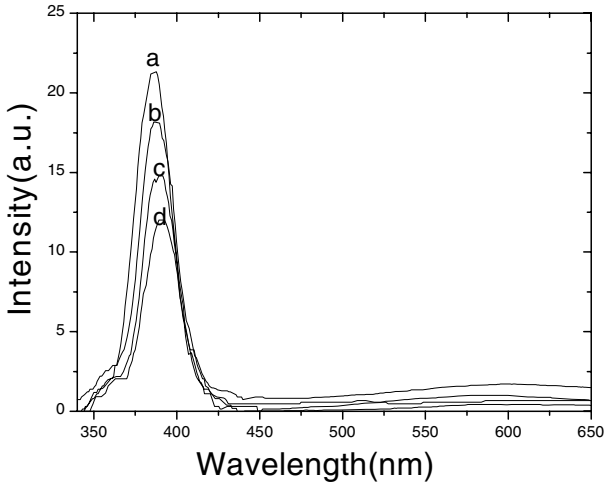

Figure 7. RT PL spectra of ZnO nanoparticles. (a) Heated at 160 °C for 2 h, then aged at 180 °C for 16 h. (b)–(d) Heated at 200, 250, and 300 °C, respectively, for 3 h.

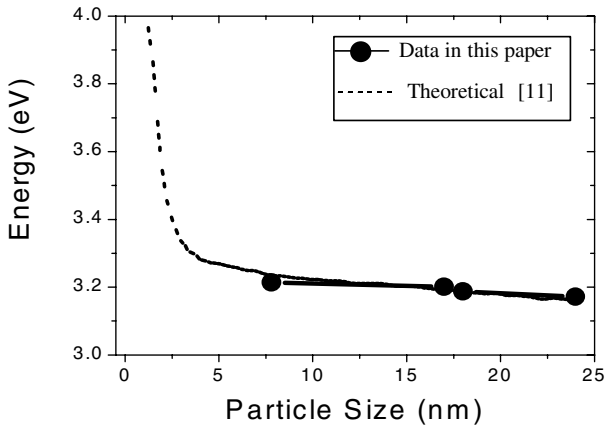

Figure 8. The comparison between the theoretical ZnO quantum size effect and the ZnO experimental data.

Room temperature PL spectra are shown in figure 7. The PL spectra exhibit strong near-band-edge emission at 386–391 nm with a full width at half-maximum about 22 nm. The PL peaks from 386 to 391 nm derive from the quantum size effect. We also note that the PL intensity of the ZnO nanoparticles increases with decreasing crystallite size. This results from the quantum size effect. According to the previous report [12], the PL peaks are attributable to bound excitons. Bound excitons related to Li^+ or Na^+ centres [18, 19] in ZnO have been reported by several groups before. Na^+ is inevitably a dopant in our ZnO nanoparticles since we used $NaHCO_3$ in the synthesis precursors. It is also interesting to note that the PL spectrum with strong UV emission was observed while the visible emission was nearly fully quenched. This is a result of the fine quality of the ZnO nanoparticles synthesized at low temperature. High temperature can lead to considerable constraints on combining the desirable characteristics of ZnO nanopowders. High-temperature processing also causes visible emission. Figure 8 shows the dependence of the band-gap enlargement on the particle diameter. The figure shows the comparison between the theoretical ZnO quantum size effect and the ZnO data from figure 7 and table 1 in this paper [11]. It shows that the ZnO experimental data basically agree with the theoretical results.

4. Summary

In summary, the low-temperature solid-state thermal decomposition process proposed here expands the range of ZnO nanoparticle synthesis methods. This novel route is focused on a strategy for separating these nanoparticles by using the by-product CH_3COONa formed, which can distribute on the nanoparticle surfaces to prevent the ZnO from agglomerating; the by-product CH_3COONa is easy to remove. TEM, XRD, IR, and Raman scattering were used to characterize the ZnO nanoparticles. Optical properties of ZnO nanoparticles have also been investigated. The nanocrystalline ZnO shows only strong UV emission, which was a result of the fine quality of the ZnO nanoparticles.

Acknowledgments

This project was supported by the Innovation Funds of the Chinese Academy of Sciences. We wish to thank Professor Zhongsu Guan and other members for their assistance in using XRD, TEM, IR, XPS, TDA and PL facilities.

References

[1] Hachigo A, Nakahata H, Higaki K, Fujii S and Shikata S-I 1994 *Appl. Phys. Lett.* **65** 2556
[2] Morkoc H, Strite S, Cao G B, Lin M E and Sverdlov B 1994 *J. Appl. Phys.* **76** 1363
[3] Cao H, Xu J Y and Zhang D Z 2000 *Phys. Rev. Lett.* **84** 5584
[4] Bagnall D M, Chen Y F, Shen M Y, Zhu Z, Goto T and Yao T 1998 *J. Cryst. Growth* **184/185** 605
[5] Spanhel L and Anderson M A 1991 *J. Am. Chem. Soc.* **113** 2826
[6] Meulenkamp E A 1998 *J. Phys. Chem.* B **102** 5566
[7] Van Dijken A, Meulenkamp E A, Vanmaekelbergh D and Meijerink A 2000 *J. Phys. Chem.* B **104** 1715
[8] Izaki M and Omi T 1996 *Appl. Phys. Lett.* **68** 2439
[9] Wong E M and Searson P C 1999 *Appl. Phys. Lett.* **74** 2939
[10] Liu Run, Vertegel A A, Bohannan E W, Sorenson T A and Switzer J A 2001 *Chem. Mater.* **13** 508
[11] Wong E M and Searson P C 1999 *Appl. Phys. Lett.* **74** 2939
[12] Yang C L, Wang J N and Ge W K 2001 *J. Appl. Phys.* **90** 4489
[13] Xu Dongsheng, Shi Xuesong, Guo Guolin, Gui Linlin and Tang Youqi 2000 *J. Phys. Chem.* B **104** 5061
[14] Kortan A R *et al* 1990 *J. Am. Chem. Soc.* **112** 1327
[15] Brus L E 1984 *J. Chem. Phys.* **80** 4403
[16] Tzolov M, Tzenov N, Dimova-Malinovska D, Kalitzova M, Pizzuto C, Vitali G, Zollo G and Ivanov I 2000 *Thin Solid Films* **379** 28
[17] Scott J F 1970 *Phys. Rev.* B **2** 1209
[18] Klingshirn C 1975 *Phys. Status Solidi* b **71** 547
[19] Reynolds D C, Litton C W and Collins T C 1969 *Phys. Rev.* **185** 1099